THE JOURNAL OF BIOLOGICAL CHEMISTRY
Vol. 276, No. 46, Issue of November 16, pp. 42978–42985, 2001
Printed in U.S.A.

Ubiquitination Precedes Internalization and Proteolytic Cleavage of Plasma Membrane-bound Glycine Receptors*

Received for publication, March 8, 2001, and in revised form, September 7, 2001
Published, JBC Papers in Press, September 17, 2001, DOI 10.1074/jbc.M102121200

Cora Büttner‡, Sven Sadtler‡, Anne Leyendecker‡, Bodo Laube§, Nathalie Griffon§¶, Heinrich Betz§, and Günther Schmalzing‡‖

From the ‡Department of Pharmacology, Biocenter of the Johann Wolfgang Goethe University, Marie Curie Strasse 9, Frankfurt am Main 60439, and the §Department of Neurochemistry, Max Planck Institute for Brain Research, Deutschordenstrasse 46, Frankfurt am Main 60528, Germany

The inhibitory glycine receptor (GlyR) in developing spinal neurones is internalized efficiently upon antagonist inhibition. Here we used surface labeling combined with affinity purification to show that homopentameric α1 GlyRs generated in *Xenopus* oocytes are proteolytically nicked into fragments of 35 and 13 kDa upon prolonged incubation. Nicked GlyRs do not exist at the cell surface, indicating that proteolysis occurs exclusively in the endocytotic pathway. Consistent with this interpretation, elevation of the lysosomal pH, but not the proteasome inhibitor lactacystin, prevents GlyR cleavage. Prior to internalization, α1 GlyRs are conjugated extensively with ubiquitin in the plasma membrane. Our results are consistent with ubiquitination regulating the endocytosis and subsequent proteolysis of GlyRs residing in the plasma membrane. Ubiquitin-conjugating enzymes thus may have a crucial role in synaptic plasticity by determining postsynaptic receptor numbers.

The efficiency of synaptic transmission depends critically on a dense packing of neurotransmitter receptors in the postsynaptic membrane. At fast synapses, ligand-gated ion channels (LGICs)[1] mediate the postsynaptic response. Different lines of evidence indicate that the distribution and density of LGICs in the plasma membrane are regulated tightly. In differentiating muscle fibers, the formation of a densely packed postsynaptic matrix of nicotinic acetylcholine receptors (nAChRs) at the developing motor endplate requires restriction of gene expression to subsynaptic nuclei, efficient internalization and degradation of extrasynaptic receptors, synaptic clustering by rapsyn, and slowing of the turnover of synaptically accumulated nAChRs (1, 2). Inversely, muscle denervation (2) or blockade of neurotransmission by α-bungarotoxin (3) causes a loss of nAChRs from the postsynaptic membrane because of an increased rate of protein turnover (4). Because nAChR degradation occurs only after internalization and lysosomal targeting of the receptor protein (4, 5), endocytosis is considered to be of crucial importance in the control of postsynaptic receptor density. An unexpectedly dynamic role of exo- and endocytosis in regulating synaptic efficacy has emerged recently from studies on glutamatergic synapses in the central nervous system (6, 7). High frequency stimulation of hippocampal neurons has been shown to trigger the plasma membrane insertion of AMPA subtype glutamate receptors in dendritic spines during long term potentiation (8), whereas receptor removal by clathrin-mediated internalization may be essential for inducing long term depression in the cerebellum (9, 10). In summary, developmental and electrical activity-driven changes in LGIC numbers appear to be based on a tight regulation of the surface incorporation and endocytotic recycling of these membrane proteins.

Another LGIC in the central nervous system known to undergo efficient endocytosis is the inhibitory glycine receptor (GlyR), a pentameric membrane protein (11, 12) that mediates postsynaptic inhibition in spinal cord and other regions of the mammalian central nervous system. Addition of the antagonist strychnine to cultured spinal neurons has been shown to cause internalization of GlyRs into an endosomal compartment (13, 14). Concomitantly, the blocked GlyRs fail to co-localize with gephyrin, a peripheral membrane protein that anchors GlyRs and $GABA_A$ receptors in the postsynaptic membrane (for review, see Ref. 15). This may indicate that anchoring to postsynaptic gephyrin protects synaptically localized GlyRs against endocytosis. Consistent with this view, in neurons from gephyrin-deficient mice a loss of $GABA_A$ receptor localization at synapses is accompanied by increased levels of intracellular receptor immunoreactivity (16).

In conclusion, there is a variety of processes in which regulated endocytosis appears to contribute significantly to the control of postsynaptic LGIC density. The mechanisms that trigger internalization are, however, not well understood. Here, we have used a recombinant homo-oligomeric GlyR generated in *Xenopus* oocytes as a model system to search for reactions involved in receptor endocytosis. The GlyR appeared to be particularly suited for such an analysis because its molecular structure, subunit assembly, and cell surface incorporation have been analyzed in detail. Presently, four GlyR genes encoding ligand-binding α subunits (α1–α4) and a single gene for

* This work was supported by Deutsche Forschungsgemeinschaft Grants SFB 474 and Schm536/2-3, the Fonds der Chemischen Industrie, and BIOMED 2 Contract BMH4-CT-97-2374. The costs of publication of this article were defrayed in part by the payment of page charges. This article must therefore be hereby marked "*advertisement*" in accordance with 18 U.S.C. Section 1734 solely to indicate this fact.

We dedicate this paper to the memory of the late Prof. Helmut Holzer and to Prof. Nobuhiko Katunuma.

¶ Present address: Unité de Neurobiologie et Pharmacologie Moléculaire, INSERM U109, Center Paul Broca, 2ter rue d'Alesia, Paris 75014, France.

‖ Present address: Dept. of Molecular Pharmacology, Technical University of Aachen, Wendlingweg 2, Aachen D-52074, Germany. To whom correspondence should be addressed. Tel.: 49-241-808-9130; Fax: 49-241-888-8433; E-mail: gschmalzing@post.klinikum.rwth-aachen.de.

[1] The abbreviations used are: LGIC(s), ligand-gated ion channel(s); nAChR(s), nicotinic acetylcholine receptor(s); AMPA, α-amino-3-hydroxy-5-methyl-4-isoxazole propionic acid; GlyR(s), inhibitory glycine receptor(s); $GABA_A$ and $GABA_C$, γ-aminobutyric acid types A and C, respectively; BN, blue native; PAGE; polyacrylamide gel electrophoresis; sulfo-SHPP, sulfosuccinimidyl-3-(4-hydroxyphenyl)proprionate; Ni^{2+}-NTA, nickel-nitrilotriacetic acid; Tricine, *N*-[2-hydroxy-1,1-bis(hydroxymethyl)ethyl]glycine; ER, endoplasmic reticulum; Endo H, endoglycosidase H; PNGase F, peptide *N*-glycosidase F.

the structural β subunit are known in vertebrates (for review, see Refs. 17 and 18). These subunits form homo-oligomeric and hetero-oligomeric chloride channels in different regions of the mammalian central nervous system. Each subunit shares with the other members of the nAChR superfamily a large glycosylated N-terminal ectodomain and four membrane-spanning regions (M1–M4), which, between M1 and M3, are separated by short hydrophilic stretches, and between M3 and M4 by a loop of ~85 amino acids (β subunit 124 amino acids) which faces the cytosol. All α subunit isoforms assemble into functional homopentameric GlyR upon heterologous expression in *Xenopus* oocytes or mammalian cells (19–21). This assembly occurs soon after polypeptide synthesis in the endoplasmic reticulum and is a prerequisite for efficient export to the cell surface (21). By using affinity purification combined with selective cell surface labeling and blue native (BN) polyacrylamide gel electrophoresis (PAGE), we now show that the recombinant GlyR is targeted to internalization and degradation after selective ubiquitination at the plasma membrane. Conjugation to ubiquitin is known to serve as an internalization signal for other receptor and ion channel proteins (22, 23). Our data thus suggest that ubiquitin-conjugating enzymes may have a crucial role in regulating postsynaptic LGIC densities.

EXPERIMENTAL PROCEDURES

Materials and Antibodies—Sulfosuccinimidyl-3-(4-hydroxyphenyl) proprionate (sulfo-SHPP) was from Pierce. Concanamycin and lactacystin were from Alexis Biochemicals (San Diego, CA). A rabbit antiserum and a monoclonal antibody to ubiquitin were purchased from Santa Cruz Biotechnologies (La Jolla, CA) and Chemicon (Temecula, CA), respectively.

cDNA Constructs—All amino acids were numbered according to their position in the mature protein sequence. cDNA constructs encoding α1-His with a C-terminal hexahistidyl tag (His) have been described before (21). Lysine 411 was mutated to arginine (mutant K411R) using the QuikChange site-directed mutagenesis kit (Stratagene), and the mutation was confirmed by sequencing. cDNA encoding human ubiquitin (24) was amplified by reverse transcription-polymerase chain reaction from a human brain cDNA library (Life Technologies, Inc.) using gene-specific primers (forward, 5′-AAAgacgtcGAAGTAGCCAGAATGCAGATCTTCGTGAAGACTCTGACTGGTAA; reverse, 5′-TTGAATTCTGCCCATTATCAACCCCCCCTCAAGCGCA) cloned into the vector pNKS2 (25) and sequenced. The forward polymerase chain reaction primer contained unique restriction sites for *Aat* II (lower case letters) and *Bsm* I (underlined) at the start codon. Taking advantage of these sites, codons for a N-terminal hexahistidyl tag were inserted to generate His-ubiquitin (His tag at the N terminus).

cRNA Synthesis and Oocyte Expression—Capped cRNAs were synthesized from linearized templates with SP6 RNA polymerase (Amersham Pharmacia Biotech) and purified as described (26). For oocyte injection, the cRNAs were dissolved in 5 mM Tris/HCl, pH 7.5, at 0.5 μg/μl, using the absorbance reading at 260 nm for quantitation (A 1.0 = 40 μg/μl). Defolliculated *Xenopus* oocytes of oogenesis stage V or VI (26) were injected with about 50-nl aliquots of cRNAs. Oocytes were kept at 19 °C in sterile frog Ringer's solution (90 mM NaCl, 1 mM KCl, 1 mM $CaCl_2$, 1 mM $MgCl_2$, and 10 mM Hepes, pH 7.4) supplemented with 50 mg/liter gentamycin. One to 3 days after cRNA injection, macroscopic glycine responses were measured by two-electrode voltage clamp recording at a holding potential of −70 mV as described previously (12).

Protein Purification, BN-PAGE, and SDS-PAGE—cRNA-injected oocytes and noninjected controls were labeled metabolically by overnight incubation with L-[^{35}S]methionine (>40 TBq/mmol, Amersham Pharmacia Biotech) at about 100 MBq/ml (0.1 MBq/oocyte) in frog Ringer's solution at 19 °C and chased with 1 mM unlabeled methionine as indicated. Oocytes expressing His-ubiquitin were preincubated at 10 mM *N*-ethylmaleimide to inactivate ubiquitin proteases prior to cell lysis. His-tagged proteins were then purified by Ni^{2+}-NTA-agarose (Qiagen) chromatography from digitonin (1%, w/v) extracts of oocytes as detailed previously (27) with the following modification. Iodoacetamide was routinely included at 10 mM and 1 mM in the lysis and washing buffers, respectively, to prevent artificial cross-linking of polypeptides by disulfide bonds. Bound proteins were released from the Ni^{2+}-NTA-agarose with nondenaturing elution buffer consisting of 0.5% (w/v) digitonin and 250 mM imidazole HCl, pH 7.6 (equivalent to 50 mM Cl^-), and kept at 0 °C until analyzed by PAGE. For selective labeling of plasma membrane receptors, the injected oocytes were incubated for 3 days at 19 °C and then labeled with freshly radioiodinated ($Na^{125}I$, Amersham Pharmacia Biotech) sulfo-SHPP (^{125}I-sulfo-SHPP), a membrane-impermeant derivative of the Bolton-Hunter reagent (28), exactly as described (27). Where indicated, surface radioiodinated oocytes were incubated for another 20 h at 19 °C after removal of unbound ^{125}I-sulfo-SHPP by washing in frog Ringer's solution. Proteins were then purified from digitonin extracts of the oocytes by Ni^{2+}-NTA-agarose chromatography as detailed above.

BN-PAGE (29) was performed as described (27). Before loading, purified proteins were supplemented with BN sample buffer to final concentrations of 10% (v/v) glycerol, 0.2% (w/v) Serva blue G, and 20 mM sodium 6-amino-*n*-caproate, and applied onto polyacrylamide gradient slab gels. Molecular mass markers (Combithek II, Roche Molecular Biochemicals) were visualized by Coomassie staining. For SDS-PAGE or Tricine-SDS-PAGE (30), proteins were supplemented with the appropriate SDS sample buffer containing 20 mM dithiothreitol (DTT) and electrophoresed in parallel with ^{14}C-labeled molecular mass markers (Rainbow, Amersham Pharmacia Biotech) on SDS-polyacrylamide gels. Where indicated, samples were treated prior to SDS-PAGE with either endoglycosidase H (Endo H) or PNGase F (New England Biolabs) in the presence of 1% (w/v) octyl glucoside to reduce inactivation of PNGase F. Gels were fixed, dried, and exposed to BioMax MR or MS film (Kodak) at −80 °C. In some experiments, radioactive bands were quantified with an image analyzer (PhosphorImager Storm 820, Molecular Dynamics).

RESULTS

Post-ER Cleavage of α1-His Subunits into Fragments of 35 and 13 kDa—After removal of the 28 amino acids of the signal peptide, the native human α1-His subunit encompasses 421+6 amino acid residues, corresponding to a calculated protein core of 49.2 kDa. The α1-His subunit migrated at an apparent mass of 48 kDa when isolated by Ni^{2+}-NTA-agarose chromatography under nondenaturing conditions from *Xenopus* oocytes and analyzed by reducing Tricine-SDS-PAGE after a 6-h [^{35}S]methionine pulse. Subsequent to a 20-h chase interval, an additional 35-kDa protein was isolated which was not present immediately after the pulse. To identify smaller fragments generated during cleavage of the 48-kDa full-length α1-His subunit, we used Tricine-SDS-polyacrylamide gels appropriate for resolution of low mass polypeptides. Fig. 1*A* shows that a 13-kDa polypeptide was detected consistently when α1-His GlyR was isolated after a 20-h chase interval, but not directly after the [^{35}S]methionine labeling pulse. These data indicate that the α1-His subunit is cleaved proteolytically into two defined fragments of 35 and 13 kDa during the chase period.

To determine the regions from which the two fragments originated, we exploited the fact that the α1-His subunit harbors a single *N*-linked oligosaccharide side chain at position 38 (^{38}NVS; see Fig. 7). Hence, the fragment derived from the N-terminal portion must include this unique *N*-glycan. Fig. 1*B* shows that PNGase F, which is capable of releasing complex-type carbohydrates, reduced the molecular masses of both the 48-kDa subunit and its 35-kDa fragment by ~3 kDa; this corresponds to the mass of one single *N*-linked oligosaccharide chain (21). In contrast, the mobility of the 13-kDa fragment did not increase upon PNGase F treatment. We conclude from these data that the sole *N*-glycan is located on the 35-kDa fragment, whereas the 13-kDa fragment originates from the nonglycosylated C-terminal portion of the α1-His subunit and thus carries the hexahistidyl tag.

Fig. 1*B* also shows that after a 20-h chase period none of the polypeptides was reduced in molecular mass by Endo H, which removes high mannose-type sugars characteristic for proteins that have not yet left the ER. The acquisition of Endo H resistance of virtually all full-length 48-kDa α1-His subunits during the chase is consistent with an efficient ER exit of the homopentameric receptor (21). The 35-kDa cleavage product appeared during the chase interval and existed in the complex-

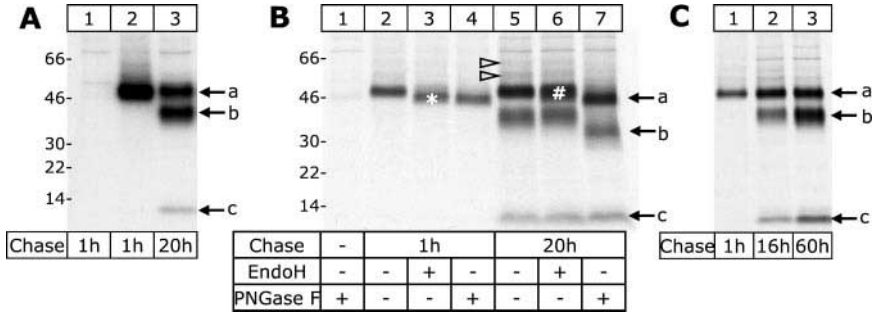

FIG. 1. **The α1-His subunit of the GlyR is cleaved outside the ER into a glycosylated 35-kDa fragment and a nonglycosylated 13-kDa fragment.** Oocytes were injected with α1-His GlyR cRNA, labeled with [^{35}S]methionine, and extracted with digitonin after the indicated chase interval. Proteins were natively purified by Ni^{2+}-NTA-agarose chromatography, denatured with Tricine-SDS sample buffer, and resolved by reducing Tricine-SDS-PAGE (4/10/13% acrylamide). The autoradiographs of the gels are shown. *Panel A*, during a 20-h chase interval, α1-His subunits within the homopentameric GlyR were cleaved into fragments of 35 and 13 kDa. *Lane 1*, noninjected control oocytes. *Panel B*, GlyRs were incubated in the presence of Tricine-SDS sample buffer, DTT, and octyl glucoside with Endo H or PNGase F for 2 h as indicated. Shortly after the pulse, α1-His subunits are largely in the Endo H-sensitive form (*) but become entirely Endo H-resistant during the chase (#). Deglycosylation with PNGase F reveals that the sole *N*-glycan of the α1-His subunit at Asn-38 is located on the 35-kDa fragment. *Lane 1*, noninjected control oocytes. *Panel C*, fragments are not degraded further upon extension of the chase interval. *a*, full-length α1-His; *b*, truncated α1-His; *c*, corresponding 13-kDa fragment.

glycosylated form only (Fig. 1*B*), indicating that the proteolytic cleavage took place outside the ER, *i.e.* within or beyond the Golgi. During prolonged chase intervals, there was a further increase in the amounts of both the 35- and 13-kDa fragments at the expense of the 48-kDa polypeptide (Fig. 1*C*). A significant fraction of the α1-His subunit remained at 48 kDa, however, even after a 60-h chase period.

The α1-His GlyR Complex Remains Assembled after Cleavage—GlyR α1 subunits assemble into a homopentamer rapidly after their synthesis while still in the ER (21). The isolation of two fragments of the full-length α1-His subunit suggested that these fragments remain associated during purification because only the 13-kDa C-terminal fragment carries the hexahistidyl tag that interacts with the Ni^{2+}-NTA beads. To examine directly whether the 13-kDa fragment is an integral part of the pentameric α1-His GlyR complex, we analyzed the natively isolated receptor by BN-PAGE before and after a 48-h chase interval, *i.e.* before and after partial cleavage. Under nondenaturing conditions, the α1-His GlyR migrated as a single protein with an apparent mass of 400 kDa irrespective of the length of the chase interval (Fig. 2*A*, *lanes 3* and *5*). The 13-kDa fragment in particular could not be detected.

Treatment of the α1-His GlyR isolated shortly after the pulse with urea and DTT to weaken noncovalent subunit interactions produced five distinct bands (Fig. 2*A*, *lane 4*), consistent with the pentameric nature of this receptor (21). If, however, the α1-His GlyR isolated after a 48-h chase interval was subjected to the same treatment, up to nine distinct bands were resolved by BN-PAGE (Fig. 2*A*, *lane 6*). To identify the individual polypeptides of which these bands were composed, the corresponding lane developed in the first dimension by BN-PAGE was excised, soaked with SDS and β-mercaptoethanol, and reanalyzed in the second dimension by reducing Tricine-SDS-PAGE (Fig. 2*B*). This analysis revealed that the 13-kDa fragment was released entirely by treatment with DTT/urea and corresponded to band 9 on the BN-polyacrylamide gel (Fig. 2*A*). In addition, the 35-kDa and 48-kDa polypeptides could be clearly attributed to bands 8 and 7, respectively, on the BN-polyacrylamide gel. Notably, the assembly intermediates consisted of multiples of either 48-kDa subunits or truncated 35-kDa subunits (Fig. 2*B*) but not a mixture of both. In other words, either the five subunits that constitute the native α1-His GlyR were all intact or all proteolytically nicked.

Truncated Forms of the α1-His GlyR Are Exclusively Intracellular—To visualize selectively the plasma membrane-bound α1-His GlyR, we radioiodinated the outer cell surface of oocytes with ^{125}I-sulfo-SHPP, a membrane-impermeant Bolton-Hunter derivative (28). Three days after cRNA injection, *i.e.* at a time when a large portion of the metabolically labeled α1-His subunits were already proteolytically nicked (Fig. 3*A*, *lane 1*), the plasma membrane contained only the full-length 48-kDa polypeptide (Fig. 3*A*, *lane 2*). This indicated that the 35-kDa product was either not routed to the cell surface or that cleavage occurred in a compartment distal from the plasma membrane (see below). Unexpectedly, however, two polypeptides of 55 and 62 kDa, and occasionally a third band of 69 kDa, were resolved by Tricine-SDS-PAGE in addition to the 48-kDa full-length α1-His subunit. Upon treatment with glycosidases, the 55- and 62-kDa polypeptides behaved exactly like authentic α1-His subunits: they were Endo H-resistant but reduced by 3 kDa upon PNGase F treatment, indicating that they all carried a single complex-type *N*-glycan (data not shown). BN-PAGE analysis of the surface radioiodinated GlyR combined with Tricine-SDS-PAGE in the second dimension revealed that the 55- and the 62-kDa polypeptides were integral parts of the α1-His pentamer (Fig. 3*B*) and not co-isolated accessory proteins. We conclude from these results that the 55- and the 62-kDa poylpeptides represent α1-His subunits of the homopentameric GlyR which were conjugated with a 7-kDa molecule en route to the plasma membrane or at the plasma membrane itself. Retrospectively, small amounts of these additional polypeptides could also be detected on autoradiographs of α1-His GlyR purified from [^{35}S]methionine-labeled oocytes (Fig. 1*B*, *open arrowheads*).

The α1 GlyR Can Be Isolated from the Cell Surface through Hexahistidyl-tagged Ubiquitin—Because the ladder of plasma membrane α1 subunit bands differing from each other by ~7 kDa was reminiscent of that of other polypeptides conjugated to one, two, and three molecules of ubiquitin, a protein of 76 amino acids, we examined whether a significant fraction of the α1-His GlyR indeed exists in ubiquitinated form at the plasma membrane. Using antibodies to ubiquitin, we were unable to detect the presence of ubiquitin in affinity-purified GlyR preparations by Western blotting; this presumably reflects the low abundance of this membrane receptor in our purified preparations. We therefore co-expressed human His-ubiquitin together with the nonhistidyl-tagged GlyR α1 subunit to examine whether GlyRs can be isolated through covalently attached His-ubiquitin. Control purifications from [^{35}S]methionine-labeled oocytes confirmed that His-ubiquitin was synthesized efficiently in oocytes (see Fig. 4*C*). Using this co-expression approach, nontagged α1 GlyR was purified through His-tagged

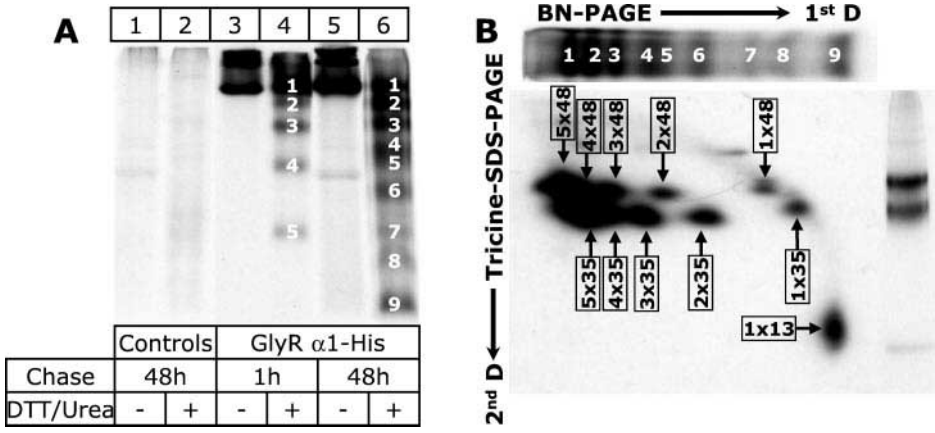

FIG. 2. **Analysis of proteolytically nicked α1-His GlyR by two-dimensional PAGE.** Oocytes injected with α1-His GlyR cRNA and labeled with [^{35}S]methionine were extracted with digitonin after the indicated chase interval. Autoradiographs of the gels are shown. *Panel A*, GlyR was natively purified by Ni^{2+}-NTA-agarose chromatography and resolved by BN-PAGE either without further treatment or after a 1-h incubation at 37 °C and 100 mM DTT, 8 M urea as indicated. Incubation with DTT and urea of GlyR isolated after a 1-h chase, *i.e.* prior to intracellular cleavage, leads to five bands (numbered *1–5*, *lane 4*), whereas nine bands (numbered *1–9*, *lane 6*) are produced when the proteolytically nicked GlyR is subjected to treatment with DTT and urea. *Lanes 1* and *2* refer to noninjected oocytes that were used as controls. *Panel B*, an aliquot of the same α1-His GlyR isolated after a 48 h chase as in *panel A* was treated with DTT and urea to generate dissociation intermediates and then resolved by BN-PAGE (4–16% acrylamide) and reducing Tricine-SDS-PAGE (4/10/13% acrylamide) in the first and second dimensions, respectively. As in *panel A*, the protein bands resolved by BN-PAGE are numbered from *1* to *9*. Second dimension Tricine-SDS-PAGE identifies bands 7, 8, and 9 to correspond to monomers of 48, 35, and 13 kDa, respectively. The additionally resolved protein bands 1–6 represent homomultimers of either full-length 48-kDa α1-His subunits or truncated 35-kDa α1-His subunits. The *boxed* numbers denote the number of subunits × molecular mass/subunit of the protein resolved by BN-PAGE, which leads in the second dimension to the spot indicated by the *arrow*. Note that the 13-kDa fragment exists solely as a monomer after treatment with urea and DTT and not in a complex with any of the 35-kDa multimers, inferring that the interaction of the N-terminal 35-kDa fragments among themselves is much stronger than with the C-terminal 13-kDa fragment.

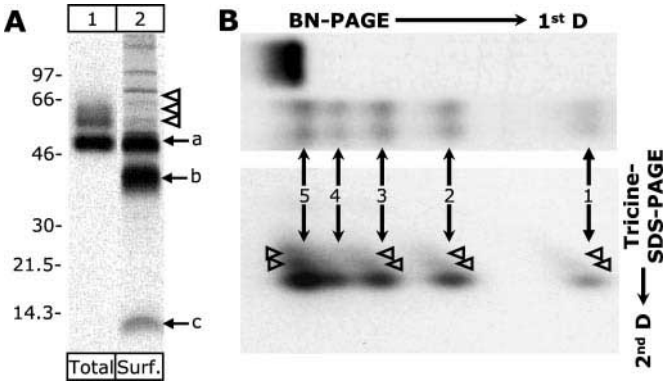

FIG. 3. **Surface GlyR lacks nicked α1-His subunits but contains 55- and 62-kDa α1-His subunits.** Three days after injection of the indicated cRNAs, oocytes were surface labeled with ^{125}I-sulfo-SHPP and extracted with digitonin. *Panel A*, proteins were purified under nondenaturing conditions by Ni^{2+}-NTA-agarose chromatography, denatured with SDS, and resolved by reducing Tricine-SDS-PAGE. For direct comparison, α1-His subunits isolated after a 6-h [^{35}S]methionine pulse and a 40-h chase are also shown (*lane 1*). *Total* and *Surf.* refer to the [^{35}S]methionine-labeled total form of the α1-His subunit and the ^{125}I-labeled surface GlyR α1-His subunit, respectively. *a*, full-length 48-kDa α1-His subunit; *b* and *c*, positions of α1-His cleavage products of 35 and 13 kDa, respectively. *Open arrowheads*, mono-, di-, and triubiquitinated α1-His subunits. *Panel B*, ^{125}I-labeled surface GlyR was treated with DTT and urea to generate assembly intermediates and then resolved by BN-PAGE (4–10% acrylamide) and reducing Tricine-SDS-PAGE (4/10/13% acrylamide) in the first and second dimensions, respectively. *Numbered arrows* indicate positions of monomeric, dimeric, trimeric, tetrameric, and pentameric GlyR α1-His displayed by first dimension BN-PAGE. In addition, the *arrows* assign the multimers and the monomer to the corresponding polypeptides resolved by second dimension Tricine-SDS-PAGE. *Open arrowheads* mark positions of 55- and 62-kDa polypeptides representing mono- and di-ubiquitinated α1-His subunits.

ubiquitin from surface-radioiodinated oocytes (Fig. 4*A*). Tricine-SDS-PAGE analysis revealed the presence of polypeptides of 55 and 62 kDa, corresponding to mono- and di-ubiquitinated forms of the 48 kDa α1 subunit (Fig. 4*A*). A major fraction of the α1 subunit existed also in the nonubiquitinated 48-kDa form and was apparently co-isolated with the ubiquitinated receptor polypeptides. This argues that not all α1 subunits within the homopentamer carried ubiquitin chains, whereas some were evidently multiply ubiquitinated. Nonhistidyl-tagged GlyR α1 subunits could also be purified from oocytes injected with a commercially available recombinant His-ubiquitin protein together with GlyR α1 cRNA (Fig. 4*B*).

From oocytes synthesizing nontagged GlyR α1 subunits without recombinant His-ubiquitin, only small amounts of GlyR protein were purified on the Ni^{2+}-NTA beads, which consistently accounted for ≤ 5% of that obtained after coinjection of His-ubiquitin. Notably, we could not co-isolate significant amounts of GlyR α1 subunits with His-ubiquitin when using this co-expression approach with [^{35}S]methionine-labeled oocytes (Fig. 4*C*). Thus, only a minor fraction of the total cellular pool of the α1 GlyR is ubiquitinated, and this ubiquitination occurs predominantly or exclusively at the plasma membrane (see Fig. 3).

The α1-His GlyR Is Cleaved after Internalization—To characterize the membrane trafficking step at which proteolysis of the α1 GlyR occurs, we first surface labeled oocytes with ^{125}I-sulfo-SHPP and then incubated these oocytes for 20 h at either 0 °C or 19 °C. Fig. 5 shows that surface α1-His subunits migrated entirely in their full-length form and as respective ubiquitin conjugates when isolated after incubation at 0 °C. However, when the oocytes were kept for 20 h at 19 °C subsequent to surface radioiodination, both the truncated 35-kDa form and the cleaved 13-kDa fragment appeared. Because these fragments were never detected at the plasma membrane directly after surface radioiodination (Fig. 4*A*), this suggests that cleavage does not take place *en route* to or at the plasma membrane itself, but in a later compartment, *i.e.* in the endocytotic pathway.

The intense radiolabeling of the 13-kDa fragment found in these surface labeling experiments was surprising in view of the presence of only a single extracellular lysine residue (Lys-411) that is located in the short tail region just behind the fourth transmembrane domain (see Fig. 7). In contrast, the extracellularly exposed N-terminal half of the α1-His subunit

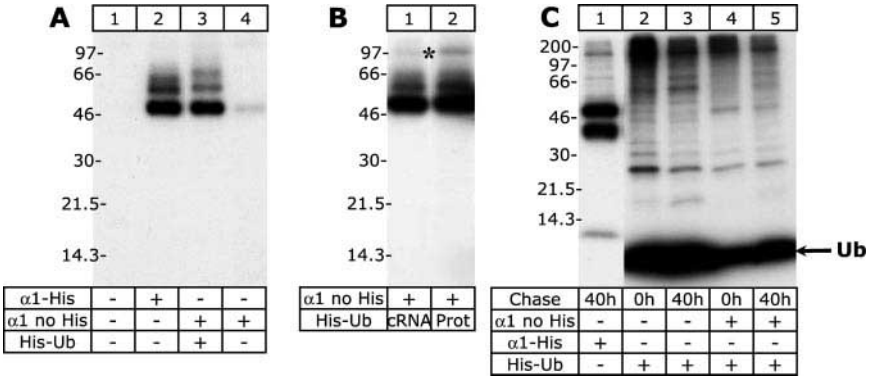

FIG. 4. **GlyR α1 is ubiquitinated at the plasma membrane.** Autoradiographies of reducing Tricine-SDS-polyacrylamide gels are shown. *Panels A* and *B*, 3 days after injection of the indicated cRNAs, oocytes were surface labeled for 1 h at 0 °C with ^{125}I-sulfo-SHPP. Oocytes were immediately extracted with digitonin, and proteins were purified under nondenaturing conditions by Ni^{2+}-NTA-agarose chromatography. The nontagged GlyR α1 subunit (*α1 no His*) could be isolated in large amounts in both His-ubiquitinated and nonubiquitinated form upon co-expression of His-ubiquitin (*panels A* and *B*) or co-injection of recombinant His-ubiquitin protein (*His-Ub prot*, *panel B*). * indicates a protein band that was also isolated from noninjected control oocytes in this particular experiment. *Panel C*, proteins were purified by Ni^{2+}-NTA-agarose chromatography from [^{35}S]methionine-labeled oocytes injected with the indicated cRNAs. Note that *lanes 4* and *5* show solely small amounts of nonubiquitinated GlyR α1 subunit but no His-ubiquitinated GlyR α1 subunit co-isolated with His-ubiquitin. *Ub*, His-ubiquitin.

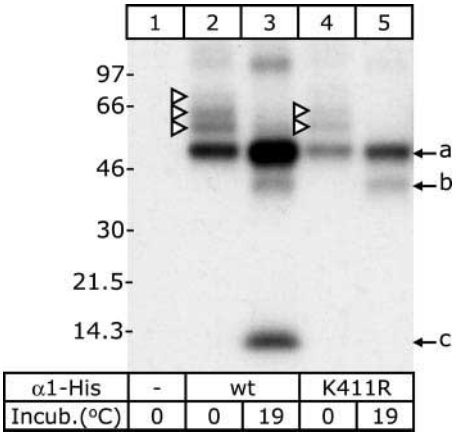

FIG. 5. **Ubiquitinated GlyR α1-His is proteolyzed after internalization.** Oocytes injected with GlyR α1-His cRNA and labeled 3 days later with ^{125}I-sulfo-SHPP were incubated further either at 0 °C or at 19 °C as indicated. After 20 h at either temperature, α1-His receptors were isolated under nondenaturing conditions by Ni^{2+}-NTA-agarose chromatography, denatured with Tricine-SDS sample buffer, and resolved by reducing Tricine-SDS-PAGE (4/10/13% acrylamide). *a*, full-length α1-His subunit of 48 kDa; *b* and *c*, positions of α1-His cleavage products of 35 and 13 kDa, respectively. Note that the 35- and 13-kDa fragments are not present at the plasma membrane of oocytes kept on ice, but appear when oocytes were kept for 20 h at 19 °C. The 13-kDa fragment remained invisible when Lys-411 of the α1-His subunit was replaced by Arg. This indicates that Lys-411 represents the sole residue at which ^{125}I-sulfo-SHPP labeling occurred at the C-terminal end of the α1-His subunit. *Open triangles* indicate ubiquitinated α1-His carrying one to three ubiquitin chains.

carries a total of 12 lysine residues that all might react with ^{125}I-sulfo-SHPP. To unravel whether Lys-411 is indeed a preferred site of iodination, we mutated this residue to arginine and purified the resulting mutant GlyR after surface radioiodination. Fig. 5 (*lane 5*) shows that the K411R mutation did not prevent the cleavage of the surface-radioiodinated full-length α1-His subunit upon subsequent incubation of the oocytes at 19 °C, as the 35-kDa band was clearly detected. The corresponding 13-kDa fragment, however, remained invisible, evidently as a result of Lys-411 elimination. Functionally, the Arg-411 α1-His GlyR was indistinguishable from its parent α1-His GlyR as assessed by two-electrode voltage clamp measurements (results not shown). These data confirm that Lys-411 is particularly accessible to covalent modification.

Cleavage of α1-His GlyR Is Blocked by Elevation of Vesicular pH but Not by a Proteasome Inhibitor—The role of endosomal or lysosomal compartments in the cleavage of α1-His GlyR was assessed further by using chemical inhibitors. Concanamycin, a specific inhibitor of vesicular H^+-ATPases similar to bafilomycin A1, has been reported to block the acidification of endosomes and lysosomes and to interfere with early to late endosomal transport (31). Incubation of oocytes in the presence of concanamycin greatly reduced the formation of the 35- and 13-kDa cleavage products (Fig. 6*A*), corroborating the view that cleavage occurs in the endocytotic pathway. Likewise, cleavage of α1-His was abolished upon addition of the lysosomotropic amine NH_4Cl (Fig. 6*A*), which dissipates transmembrane H^+ gradients of acidic organelles (32), thereby inhibiting the activity of lysosomal enzymes (33). The routing of α1-His GlyR toward the cell surface was not affected notably by concanamycin or NH_4Cl, as assessed by the unimpaired acquisition of complex-type carbohydrates in the presence of either compound (results not shown). A complete inhibition of α1-His cleavage was also seen in the presence of the serine protease inhibitor phenylmethylsulfonyl fluoride (Fig. 6*B*), which, unlike conventional lysosomal inhibitors such as NH_4Cl, does not raise lysosomal pH values. Together these data show that lysosomal serine protease activity is required for efficient cleavage of the α1-His GlyR.

Certain mammalian membrane proteins that become ubiquitinated at the plasma membrane appear to be subsequently degraded by both the lysosome and the proteasome system (34). Proteasome activity seems to be required even for endocytosis and subsequent lysosomal degradation of proteins that do not become ubiquitinated, such as the growth factor receptor (35) and the cytokine interleukin-2 receptor (36). To examine whether proteasomes contribute to the degradation of GlyR α1-His, we employed the proteasome inhibitor lactacystin. Even in the continued presence of 5 μM lactacystin, the absolute amounts of the full-length subunit and of its 35- and 13-kDa cleavage products remained unchanged (Fig. 6*C*). PhosphorImaging analysis indicated that 26 and 24% of the total α1-His were in the uncleaved 48-kDa form in the absence and presence of lactacystin, respectively. These data argue against an involvement of the proteasome in the proteolytic cleavage of the α1-His receptor.

DISCUSSION

In this paper, we show that recombinant GlyRs generated in *Xenopus* oocytes are internalized and cleaved proteolytically into defined fragments after ubiquitination at the plasma membrane. Based on these data we propose that ubiquitin

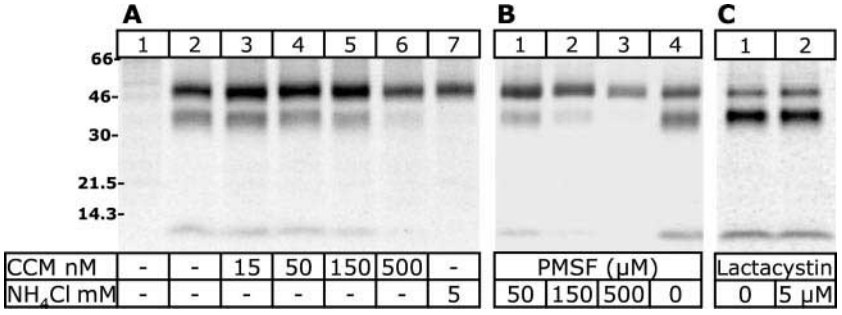

FIG. 6. **GlyR α1-His proteolysis is blocked by concanamycin, NH_4Cl, and phenylmethylsulfonyl fluoride, but not by lactacystin.** α1-His cRNA-injected oocytes were labeled with [^{35}S]methionine for 4 h and chased for 20 h in the absence and presence of the indicated concentrations of concanamycin A (*CCM*) or NH_4Cl (*panel A*), phenylmethylsulfonyl fluoride (*PMSF*, *panel B*), or lactacystin (*panel C*). Proteins were natively purified by Ni^{2+}-NTA-agarose chromatography, denatured with Tricine-SDS sample buffer, and resolved by reducing Tricine-SDS-PAGE (4/10/13% acrylamide). Autoradiographs of the gels are shown.

conjugation reactions may play a key role in the regulation of LGIC dynamics underlying synaptic development and plasticity. Although this suggestion relies at the moment entirely on *Xenopus* oocytes as host cells, it should be mentioned that an apparently identical and developmentally regulated truncation of the GlyR α1 subunits has been previously observed to occur in native neural tissue as well (37). This indicates that the oocyte system represents a useful model system to examine this particular aspect of GlyR regulation. Data obtained with oocytes will therefore be helpful to tackle questions of receptor metabolism in intact neurons.

Ubiquitination of the α1 GlyR: A Targeting Signal for Internalization and Lysosomal Degradation?—The results presented in this study show that the recombinant human α1 GlyR is ubiquitinated at the plasma membrane of *Xenopus* oocytes. Ubiquitination could be demonstrated by co-isolation of the nontagged α1 GlyR through hexahistidyl-tagged ubiquitin and by the identification of α1 subunit conjugates that differed in apparent molecular mass by ~7 kDa from each other. Mono-, di-, and tri-ubiquitinated α1 subunits within the GlyR homopentamer as visualized by surface radioiodination were prominent at the cell surface but hardly detected in total cell homogenates. Thus, ubiquitination of α1 GlyRs occurs largely or exclusively at the plasma membrane and not during intracellular routing of the receptor. Subsequent to internalization, the α1 subunits within the homopentameric GlyR complex were proteolytically nicked into an N-terminal glycosylated fragment of 35 kDa and a C-terminal fragment of 13 kDa. This nicking did, however, not impair affinity purification of the homopentameric GlyR complex, indicating that cleavage of the α1 subunits distal to M3 does not cause dissociation of fragments from the assembled receptor prior to treatment with urea or SDS. This observation agrees well with previous results showing that the extracellular N-terminal domains of GlyR subunits harbor crucial determinants of subunit assembly (12). The importance of the extracellular portion of LGIC subunits for receptor assembly has similarly been demonstrated for $GABA_A$ and $GABA_C$ receptors (38) as well as for the muscle nAChR (39). Also, the proteolytically nicked nAChR has been shown to be remarkably resistant to disassembly. Fragments produced by papain treatment of intact nAChR remained physically and functionally associated (40, 41). Even extensive proteolysis had no dramatic effect on sedimentation characteristics, toxin binding, the doughnut-like appearance in transmission electron microscopy, or cation channel function. By analogy, the nicked α1 GlyR may be able to function as a glycine-gated Cl^- channel, but apparently it is not localized in the plasma membrane. Collectively, our findings place the α1 GlyR into an abundant class of mammalian and yeast membrane proteins that, upon ubiquitination at the cell surface, are targeted into the endocytotic pathway; usually, endocytosis is followed by lysosomal or lysosomal-like vacuolar degradation (for review, see Ref. 42). This is consistent with growing evidence that ubiquitination at the plasma membrane may function as a general internalization signal to trigger the down-regulation of different receptor and channel proteins (22, 42).

Ubiquitination is well established as a major targeting signal for the recognition and degradation of short lived cytosolic proteins by the 26 S proteasome (43). In addition, ubiquitination followed by proteasomal destruction provides for degradation of many luminal and transmembrane ER proteins that, when abnormally folded or incompletely assembled, are translocated back into the cytosol (42). Among the proteins undergoing ER-associated proteasomal degradation are also unassembled subunits of multiprotein complexes. Hence, the ubiquitination of GlyR α1 subunits observed here could be a consequence of overexpression and ensuing retention of large amounts of unassembled α1 subunits in the ER. However, several lines of evidence argue against this view. First, our pulse-chase experiments clearly show that newly synthesized GlyR α1 subunits homo-oligomerize with high efficiency in the ER of *Xenopus* oocytes and, once assembled, are translocated efficiently to the Golgi, as judged from the rapid and complete acquisition of complex-type carbohydrates. Second, the homopentameric α1 GlyR is metabolically stable in *Xenopus* oocytes (half-life in the range of days) compared with incompletely folded or unassembled proteins that are targeted to the proteasome and have in general a very short half-life of <1 h. Third, we have shown that the ubiquitin-conjugated α1 subunits are contained within the assembled homopentameric GlyR complex and carry a complex-type carbohydrate chain indicative of a localization in the Golgi or later compartments. Moreover, our differential labeling experiments indicate that ubiquitination of the α1 GlyR is topologically restricted to the plasma membrane rather than occurring *en route* to the cell surface. Fourth, the proteasome inhibitor lactacystin did not increase α1-His subunit levels or inhibit α1-His cleavage. In contrast, cleavage appears to be mediated by lysosomal serine proteases because phenylmethylsulfonyl fluoride blocked processing almost as efficiently as NH_4Cl. In this respect, degradation of GlyR α1 also differs from degradation of the epithelial Na^+ channel ENaC, which involves the proteasome, but not lysosomes (44). Finally, the ubiquitinated GlyR carries only one to three ubiquitin molecules per α1 subunit; this contrasts the polyubiquitinated high molecular weight adducts routinely seen with proteins targeted for proteasomal degradation. To account for the addition of up to three ubiquitin molecules per α1 subunit, we assume that multiple lysine residues within the large cytoplasmic loop of the α1 subunit (Fig. 7) are mono-ubiquitinated, rather than that a single lysine residue carries a

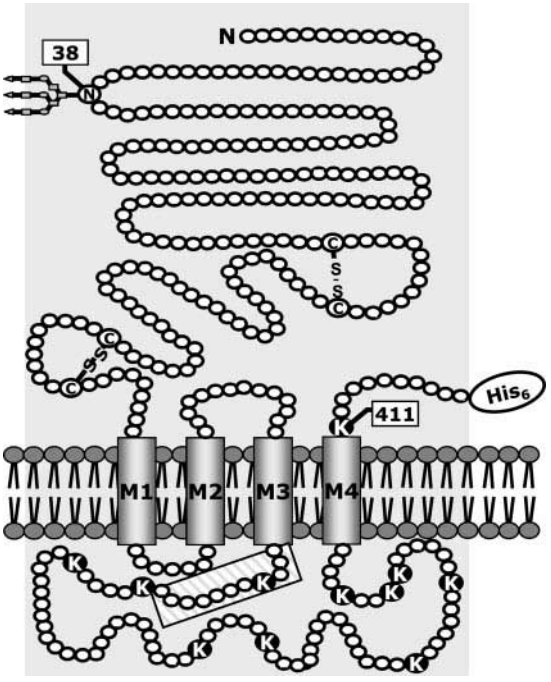

FIG. 7. **Membrane topology of the GlyR α1 subunit.** The sole *N*-glycosylation site at asparagine 38 (*N38*) and the approximate position of the cytoplasmic α1-His cleavage site (*boxed*) within the endodomain (85 amino acids) are indicated. Mutation of the extracellularly located uttermost C-terminal lysine residue (*K411*) to arginine prevents labeling of the 13-kDa C-terminal fragment by ^{125}I-sulfo-SHPP. The 10 lysine residues (*K*) within the endodomain represent putative sites for ubiquitination. *M1–M4*, membrane-spanning segments; *His$_6$*, C-terminal hexahistidyl tag.

branched multiubiquitin chain. Mono-ubiquitination has been shown to be sufficient for internalization of yeast membrane proteins, such as Ste2p, a G protein-coupled receptor (45), or the maltose transporter, a protein with 12 transmembrane segments (46). Also, ubiquitin conjugation has been shown to promote endocytosis in the absence of any other internalization signal (47). Conversely, modification by a single ubiquitin molecule or by multiple single ubiquitins on multiple distinct lysine residues is not sufficient to serve as a proteasomal targeting signal because recognition by the proteasome requires branched multiubiquitin chains containing at least four copies of ubiquitin (48). We therefore conclude that the ubiquitination reactions identified here serve exclusively in labeling GlyRs for removal from the plasma membrane.

The human GlyR α1 subunit harbors 10 cytoplasmic lysine residues, which are all located in the large intracellular loop between transmembrane segments M3 and M4 (Fig. 7). These 10 lysine residues are exposed to the cytosol not only at the plasma membrane, but also during intracellular trafficking of the GlyR. The enzymes of the ubiquitin system evidently are able to discriminate structurally the cytoplasmic GlyR loop from the many other substrates that are ubiquitinated in the same cellular compartment and to distinguish topologically GlyRs present at the cell surface from those *en route* to the plasma membrane. Ubiquitin can be transferred directly from a ubiquitin-charged ubiquitin-conjugation enzyme (denoted E2) to a substrate protein, with specificity in substrate recognition being provided by a large number of E3 ubiquitin-protein ligases. A candidate E3 molecule for ubiquitination of neuronal plasma membrane proteins including the GlyR is Nedd4 (neuronal precursor cells expressed developmentally down-regulated 4; for review, see Ref. 23), which upon overexpression in *Xenopus* oocytes, has been shown to decrease epithelial Na^+ channels numbers in the plasma membrane efficiently (49).

Potential Roles of Receptor Ubiquitination in Synaptic Development and Remodeling—Ubiquitination may serve as a general mechanism for targeting GlyRs and related LGICs to endocytosis and lysosomal degradation and thus for regulating surface receptor numbers during development and at the adult synapse. In developing muscle, extrasynaptic nAChRs are removed from the noninnervated sarcolemmal membrane rapidly, whereas synaptic receptors become metabolically stable upon further development of the neuromuscular junction (2). In contrast, during withdrawal of nerve terminals from the motor endplate the postsynaptic membrane is depleted of nAChRs before there is any obvious loss of membrane in the overlying motor nerve ending (50). A similar early loss of postsynaptic nAChRs also takes place during synapse elimination in reinnervated adult muscle (51). Notably, ubiquitin has been reported to be highly concentrated in postsynaptic membranes of neuromuscular junctions with a distribution identical to that of nAChR (52). Moreover, a rise in cytosolic ubiquitin occurs early in response to axonal injury (53). These data are consistent with ubiquitination being important in synaptic processes that require enhanced rates of receptor internalization and/or degradation.

Another process in which regulation of endocytosis by ubiquitination could play a crucial role is that of changes in receptor isoforms during development. At the neuromuscular junction, the γ subunit of the embryonic nAChR is replaced postnatally by the ϵ subunit of the adult receptor (54). Similar isoform switches occur also with glutamate, $GABA_A$, and glycine receptors in the developing central nervous system (for references, see 55). At glycinergic synapses in spinal cord, replacement of α2 homo-oligomeric neonatal GlyRs by $\alpha1\beta$ adult-type receptors accounts for the shortening of the decay of inhibitory postsynaptic currents during the first 2 postnatal weeks (56, 57). Also, electrical silencing of embryonic GlyRs by the selective antagonist strychnine causes internalization of the receptors into an endosomal compartment by an as yet unidentified pathway (13). This is consistent with an activity-dependent regulation of GlyR numbers via an endocytotic mechanism. A similar regulation of receptor internalization by synaptic activity may also be important in long term depression of excitatory synapses. In the cerebellum (9, 58) and in hippocampal neurons (10), long term depression is known to be accompanied by a reduction in AMPA receptor numbers at synaptic sites.

An important consequence of ubiquitin additions to LGIC subunits may be the disruption of protein-protein interactions at the synapse. The GlyR β subunit is known to bind the receptor-anchoring protein gephyrin via the hydrophobic side of an amphipathic sequence (amino acids 395–411) within its large cytoplasmic loop (59, 60), and this interaction is thought to be crucial for the postsynaptic localization of the receptor (15, 60, 61). Recruitment of an E3 ligase to one or several α1 subunits within an $\alpha1_3\beta_2$ heteropentameric GlyR (11) may sterically affect GlyR-gephyrin interactions and even result in ubiquitination of one or several of the 13 lysine residues within the large cytoplasmic loop of a neighboring β subunit. Conceivably, such modification might interfere with GlyR anchoring to postsynaptic gephyrin and thus facilitate receptor internalization by endocytosis. Conversely, immobilization of plasma membrane-bound heteromeric GlyRs on a preassembled gephyrin scaffold (15, 62) could protect receptors against ubiquitination and thus stabilize the postsynaptic receptor pool at the synapse (63). This hypothesis is consistent with results obtained on cultured hippocampal neurons from gephyrin-deficient mice, in which the intracellular immunoreactivities of subunits of another gephyrin-anchored receptor, the $GABA_A$ receptor, were found to be strikingly increased compared with

wild-type cells (16). Similarly, the reduction of synaptic AMPA receptor numbers seen upon induction of long term depression in cerebellar neurons is thought to involve release from the postsynaptic anchoring protein GRIP and subsequent clathrin-dependent endocytosis (58, 64).

In conclusion, all presently available data can be reconciled with the view that ubiquitination of plasma membrane LGICs constitutes an important signal in targeting receptors to intracellular compartments for proteolytic degradation and that receptor-protein interactions at the synapse may regulate receptor turnover by affecting ubiquitination reactions. The observation that multiple membrane proteins of unknown identity are conjugated with ubiquitin in brain synaptic membranes and postsynaptic densities lends further support to the idea that ubiquitination of membrane proteins is a widespread phenomenon in the mammalian brain (65).

REFERENCES

1. Colledge, M., and Froehner, S. C. (1998) *Curr. Opin. Neurobiol.* **8,** 357–363
2. Sanes, J. R., and Lichtman, J. W. (1999) *Annu. Rev. Neurosci.* **22,** 389–442
3. Akaaboune, M., Culican, S. M., Turney, S. G., and Lichtman, J. W. (1999) *Science* **286,** 503–507
4. Xu, R., and Salpeter, M. M. (1999) *J. Cell. Physiol.* **181,** 107–112
5. Pumplin, D. W., and Fambrough, D. M. (1982) *Annu. Rev. Physiol.* **44,** 319–335
6. Turrigiano, G. G. (2000) *Neuron* **26,** 5–8
7. Lüscher, C., Nicoll, R. A., Malenka, R. C., and Muller, D. (2000) *Nat. Neurosci.* **3,** 545–550
8. Shi, S. H., Hayashi, Y., Petralia, R. S., Zaman, S. H., Wenthold, R. J., Svoboda, K., and Malinow, R. (1999) *Science* **284,** 1811–1816
9. Wang, Y. T., and Linden, D. J. (2000) *Neuron* **25,** 635–647
10. Man, Y. H., Lin, J. W., Ju, W. H., Ahmadian, G., Liu, L., Becker, L. E., Sheng, M., and Wang, Y. T. (2000) *Neuron* **25,** 649–662
11. Langosch, D., Thomas, L., and Betz, H. (1988) *Proc. Natl. Acad. Sci. U. S. A.* **85,** 7394–7398
12. Kuhse, J., Laube, B., Magalei, D., and Betz, H. (1993) *Neuron* **11,** 1049–1056
13. Kirsch, J., and Betz, H. (1998) *Nature* **392,** 717–720
14. Levi, S., Vannier, C., and Triller, A. (1998) *J. Cell Sci.* **111,** 335–345
15. Kneussel, M., and Betz, H. (2000) *Trends Neurosci.* **23,** 429–435
16. Kneussel, M., Brandstätter, J. H., Laube, B., Stahl, S., Müller, U., and Betz, H. (1999) *J. Neurosci.* **19,** 9289–9297
17. Kuhse, J., Betz, H., and Kirsch, J. (1995) *Curr. Opin. Neurobiol.* **5,** 318–323
18. Harvey, R. J., and Betz, H. (2000) *Handb. Exp. Pharmacol.* **147,** 479–497
19. Schmieden, V., Grenningloh, G., Schofield, P. R., and Betz, H. (1989) *EMBO J.* **8,** 695–700
20. Akagi, H., Hirai, K., and Hishinuma, F. (1991) *FEBS Lett.* **281,** 160–166
21. Griffon, N., Büttner, C., Nicke, A., Kuhse, J., Schmalzing, G., and Betz, H. (1999) *EMBO J.* **18,** 4711–4721
22. Hicke, L. (1999) *Trends Cell Biol.* **9,** 107–112
23. Staub, O., Abriel, H., Plant, P., Ishikawa, T., Kanelis, V., Saleki, R., Horisberger, J. D., Schild, L., and Rotin, D. (2000) *Kidney Int.* **57,** 809–815
24. Wiborg, O., Pedersen, M. S., Wind, A., Berglund, L. E., Marcker, K. A., and Vuust, J. (1985) *EMBO J.* **4,** 755–759
25. Gloor, S., Pongs, O., and Schmalzing, G. (1995) *Gene* (*Amst.*) **160,** 213–217
26. Schmalzing, G., Gloor, S., Omay, H., Kröner, S., Appelhans, H., and Schwarz, W. (1991) *Biochem. J.* **279,** 329–336
27. Nicke, A., Bäumert, H. G., Rettinger, J., Eichele, A., Lambrecht, G., Mutschler, E., and Schmalzing, G. (1998) *EMBO J.* **17,** 3016–3028
28. Thompson, J. A., Lau, A. L., and Cunningham, D. D. (1987) *Biochemistry* **26,** 743–750
29. Schägger, H., Cramer, W. A., and von Jagow, G. (1994) *Anal. Biochem.* **217,** 220–230
30. Schägger, H., and von Jagow, G. (1987) *Anal. Biochem.* **166,** 368–379
31. Woo, J. T., Shinohara, C., Sakai, K., Hasumi, K., and Endo, A. (1992) *Eur. J. Biochem.* **207,** 383–389
32. Maxfield, F. R. (1982) *J. Cell Biol.* **95,** 676–681
33. Seglen, P. O., and Gordon, P. B. (1980) *Mol. Pharmacol.* **18,** 468–475
34. Strous, G. J., and Govers, R. (1999) *J. Cell Sci.* **112,** 1417–1423
35. Strous, G. J., van Kerkhof, P., Govers, R., Rotwein, P., and Schwartz, A. L. (1997) *J. Biol. Chem.* **272,** 40–43
36. Yu, A., and Malek, T. R. (2001) *J. Biol. Chem.* **276,** 381–385
37. Becker, C. M., Hoch, W., and Betz, H. (1988) *EMBO J.* **7,** 3717–3726
38. Hackam, A. S., Wang, T. L., Guggino, W. B., and Cutting, G. R. (1997) *Neuroreport* **8,** 1425–1430
39. Verrall, S., and Hall, Z. W. (1992) *Cell* **68,** 23–31
40. Lindstrom, J., Gullick, W., Conti-Tronconi, B., and Ellisman, M. (1980) *Biochemistry* **19,** 4791–4795
41. Huganir, R. L., and Racker, E. (1980) *J. Supramol. Struct.* **14,** 13–19
42. Bonifacino, J. S., and Weissman, A. M. (1998) *Annu. Rev. Cell Dev. Biol.* **14,** 19–57
43. Hershko, A., and Ciechanover, A. (1998) *Annu. Rev. Biochem.* **67,** 425–479
44. Malik, B., Schlanger, L., Al Khalili, O., Bao, H. F., Yue, G., Price, S. R., Mitch, W. E., and Eaton, D. C. (2001) *J. Biol. Chem.* **276,** 12903–12910
45. Terrell, J., Shih, S., Dunn, R., and Hicke, L. (1998) *Mol. Cell* **1,** 193–202
46. Lucero, P., Penalver, E., Vela, L., and Lagunas, R. (2000) *J. Bacteriol.* **182,** 241–243
47. Shih, S. C., Sloper-Mould, K. E., and Hicke, L. (2000) *EMBO J.* **19,** 187–198
48. Thrower, J. S., Hoffman, L., Rechsteiner, M., and Pickart, C. M. (2000) *EMBO J.* **19,** 94–102
49. Staub, O., Gautschi, I., Ishikawa, T., Breitschopf, K., Ciechanover, A., Schild, L., and Rotin, D. (1997) *EMBO J.* **16,** 6325–6336
50. Balice-Gordon, R. J., and Lichtman, J. W. (1993) *J. Neurosci.* **13,** 834–855
51. Rich, M. M., and Lichtman, J. W. (1989) *J. Neurosci.* **9,** 1781–1805
52. Serdaroglu, P., Askanas, V., and Engel, W. K. (1992) *Neuropathol. Appl. Neurobiol.* **18,** 232–236
53. De Stefano, M. E., Squitti, R., and Toschi, G. (1998) *J. Neuropathol. Exp. Neurol.* **57,** 1000–1012
54. Mishina, M., Takai, T., Imoto, K., Noda, M., Takahashi, T., Numa, S., Methfessel, C., and Sakmann, B. (1986) *Nature* **321,** 406–411
55. Missias, A. C., Mudd, J., Cunningham, J. M., Steinbach, J. H., Merlie, J. P., and Sanes, J. R. (1997) *Development* **124,** 5075–5086
56. Hoch, W., Betz, H., and Becker, C. M. (1989) *Neuron* **3,** 339–348
57. Takahashi, T., Momiyama, A., Hirai, K., Hishinuma, F., and Akagi, H. (1992) *Neuron* **9,** 1155–1161
58. Matsuda, S., Launey, T., Mikawa, S., and Hirai, H. (2000) *EMBO J.* **19,** 2765–2774
59. Meyer, G., Kirsch, J., Betz, H., and Langosch, D. (1995) *Neuron* **15,** 563–572
60. Kneussel, M., Hermann, A., Kirsch, J., and Betz, H. (1999) *J. Neurochem.* **72,** 1323–1326
61. Kirsch, J., Meyer, G., and Betz, H. (1996) *Mol. Cell Neurosci.* **8,** 93–98
62. Sola, M., Kneussel, M., Heck, I. S., Betz, H., and Weissenhorn, W. (2001) *J. Biol. Chem.* **276,** 25294–25301
63. Changeux, J. P., and Danchin, A. (1976) *Nature* **264,** 705–712
64. Xia, J., Chung, H. J., Wihler, C., Huganir, R. L., and Linden, D. J. (2000) *Neuron* **28,** 499–510
65. Chapman, A. P., Smith, S. J., Rider, C. C., and Beesley, P. W. (1994) *Neurosci. Lett.* **168,** 238–242